Membrane Water Treatment, Vol. 4, No. 2 (2013) 143-155
DOI: http://dx.doi.org/10.12989/mwt.2013.4.2.143

Microfiltration of *Chlorella* sp.: Influence of material and membrane pore size

A.L. Ahmad*, N.H. Mat Yasin, C.J.C. Derek and J.K. Lim

School of Chemical Engineering, Engineering Campus, Universiti Sains Malaysia, Seri Ampangan, 14300 Nibong Tebal, Seberang Perai Selatan, Pulau Pinang, Malaysia

(Received August 08, 2012, Revised March 09, 2013, Accepted April 01, 2013)

Abstract. Four membranes were used to separate *Chlorella* sp. from their culture medium in cross-flow microfiltration (MF) experiments: cellulose acetate (CA), cellulose nitrate (CN), polypropylene (PP) and polyvinylidenefluoride (PVDF). It was found that the hydrophilic CA and CN membranes with a pore size of 1.2 μm exhibited the best performances among all the membranes in terms of permeation flux. The hydrophobicity of each membrane material was determined by measuring the angle between the water (liquid) and membrane (solid). Contact angle measurements showed that deionized (DI) water had almost adsorbed onto the surfaces of the CA and CN membranes, which gave 0.00° contact angle values. The PP and PVDF membranes were more hydrophobic, giving contact angle values of 95.97° and 126.63°, respectively. Although the pure water flux increased with increasing pore diameter ($0.8 < 1.2 < 3.0$ μm) in hydrophilic CA and CN membranes, the best performance in term of filtration rate for filtering a microalgae suspension was attained by membranes with a pore size of 1.2 μm. The fouled membrane pore sizes and pore blocking were inspected using a scanning electron microscope (SEM). MF with large pore diameters was more sensitive to fouling that contributed to intermediate blocking, where the size of the membrane pores is almost equivalent to that of cells.

Keywords: cross-flow microfiltration; *Chlorella* sp.; flux decline; pore blocking

1. Introduction

In recent decades, various membrane processes have been developed tailored towards a wide range of applications and their numbers will certainly increase in coming years. Common applications include concentration, purification and fractionation processes. However, today, membrane filtration has been used intensively in the separation and purification steps of biotechnological processes in order to harvest micro-organisms (Rossignol *et al.* 1999) due to its economical, efficient and energy-saving advantages (Hwang and Sz 2010).

Many studies of membrane separation using microfiltration (MF) membrane have been reported on biological suspensions. Petrusevski *et al.* (1995) examined a tangential flow filtration system for the concentration of algae in natural fresh water. A membrane with 0.45 μm pores was selected for the concentration of microalgae to limit the accumulation of unwanted water constituents and to reduce membrane fouling. Jaouen *et al.* (1999) first reported the effects of

*Corresponding author, Professor, E-mail: chlatif@eng.usm.my

shear stresses on microalgal cell suspensions (*Tetraselmis suecica*) in the various pumps of tangential MF systems. Krstic *et al.* (2001) reported some observations on the influence of operation conditions, biomass structure and feed composition during cross-flow MF of *Polyporus squamosus* fermentation broth. Babel and Takizawa (2010) observed the effects of feed concentration and transmembrane pressure (TMP) on cake resistance; whereas Dizge *et al.* (2011) studied the effects of membrane type and pore size on filtration flux.

Rossi *et al.* (2008) presented the results of the fouling phenomenon with different suspensions: fresh biomass, stressed biomass and a suspension of *Arthrospira platensis* enriched in exopolysaccharides (EPS). Certainly, fouling is the major constraint in membrane filtration. It causes a significant decline in flux and increases TMP (Makardij *et al.* 1999, Pearce 2007). Consequently, in order to improve performance and minimize the fouling phenomena, it is necessary to know the important factors affecting membrane fouling. Hwang and Huang (2009) stated in their article that the fouling mechanism and the performance of membrane filtration depended on various factors: biological polymers (e.g., proteins, carbohydrates, nucleic acids), membrane characteristics (e.g., morphology, membrane pore size, zeta potential, hydrophilic affinity), bio-macromolecular characteristics (e.g., molecular weight of biopolymers, configuration) and system operating conditions (e.g., filtration pressure, cross-flow velocity, soluble microbial products (SMP) concentration). Solute adsorption and particle interception also influenced the membrane filtration processes (Hwang and Sz 2010).

To date, there have been many publications (Petrusevski *et al.* 1995, Rossignol *et al.* 1999, Jaouen *et al.* 1999, Krstic *et al.* 2001, Rossi *et al.* 2008, Babel and Takizawa 2010, Dizge *et al.* 2011) on membrane processes for algal filtration but the constraints of membrane filtration have yet to be explored in detail. The study presented here focuses on the membrane performance of cross-flow MF in the harvesting of *Chlorella* sp. suspensions. Membrane performance (i.e., permeation flux) was investigated as a function of various membrane characteristics (i.e., different membrane materials with various pore sizes) under constant operating conditions (i.e., pressure, cells concentration and cross-flow velocity). Four different types of membranes with pore sizes ranging from 0.8 μm to 3.0 μm were used in the experiments. Fresh membranes were characterized using contact angle measurements to determine the hydrophobicity of membrane surfaces. Additionally, a scanning electron microscope (SEM) was used to inspect the membrane surfaces before and after MF.

2. Materials and methods

2.1 Microalgal suspensions

The green microalga, *Chlorella* sp., that was used in this study was cultivated in Bold's Basal Medium (BBM) in a batch culture. *Chlorella* sp. was chosen as a model alga because it is commonly found in natural water and easily cultured in the laboratory (Petrusevski *et al.* 1995).

Cell concentration was determined using a hemocytometer with an optical microscope and was correlated with the absorbance at 600 nm measured using a Shimadzu UV-1601 spectrophotometer (USA). This method has been described in our previous research (Ahmad *et al.* 2011). The fresh cultures were taken on day 9 (cell density reached 4.86×10^9 cells/ml) because this day was the point at which the cells had reached their maximal electronegative strength (Ahmad *et al.* 2012, Lim *et al.* 2012). In order to compare the performances of the membranes, all experiments were

Table 1 Main characteristic of the membranes

Membrane material	Pore diameter (μm)	Manufacturer
Cellulose acetate (CA)	0.8	Sartorius
	1.2	Sterlitech
	3.0	Sterlitech
Cellulose nitrate (CN)	0.8	Sartorius
	1.2	Sartorius
	3.0	Sartorius
Polypropylene (PP)	0.8	Milipore
Polyvinylidenefluoride (PVDF)	0.8	Milipore

carried out at the same cell concentration level. The size of the particles in suspension was measured using a CILAS model 1180 (France) laser diffraction-based particle size analyzer. The measurements were performed at a wavelength of 830 nm at scattering angle ranged from 0° to 45° under wet mode and particle sizes ranging from 0.04 to 2500 μm were obtained. Approximately 60×10^9 cells per sample were used to achieve the required obscuration of 4–6 %, and each sample was measured in triplicate. The shape of the algal cells was observed using light microscopy.

2.2 Analytical methods

In this work, the surface hydrophobicities of the newly commercialized membranes were analyzed by measuring the contact angle of DI water on the different membrane materials. The contact angle measurements were then analyzed with a computer software program, Optical Contact Angle SCA 15 (Germany). A detail of the method of contact angle measurement is provided elsewhere (Ahmad *et al.* 2010). The result of all measurements was the average of at least 10 single measurements (two angles per drop). Thus, a total of 20 angle measurements were made for each membrane sample.

The surface morphologies of the fresh and fouled membranes were observed using a Carl Zeiss Supra 35VP SEM (Germany). The non-conducting membrane samples were coated with gold before visualization. Based on the SEM images, the pores of the fresh membrane were clearly visible.

2.3 MF membranes

Four commercially available MF membranes, with different nominal pore size and 47 mm in diameter of circular membrane supplied by Milipore, Sartorius and Sterlitech, were used for comparison in this work. These membranes and their characteristics are summarized in Table 1. The membranes were immersed in DI water overnight before use in the experiments. This preparative step was done to remove any trace quantities of chemicals on the membrane surface.

2.4 Experimental procedures

The experiments were performed in a specially fabricated module for flat circular membranes,

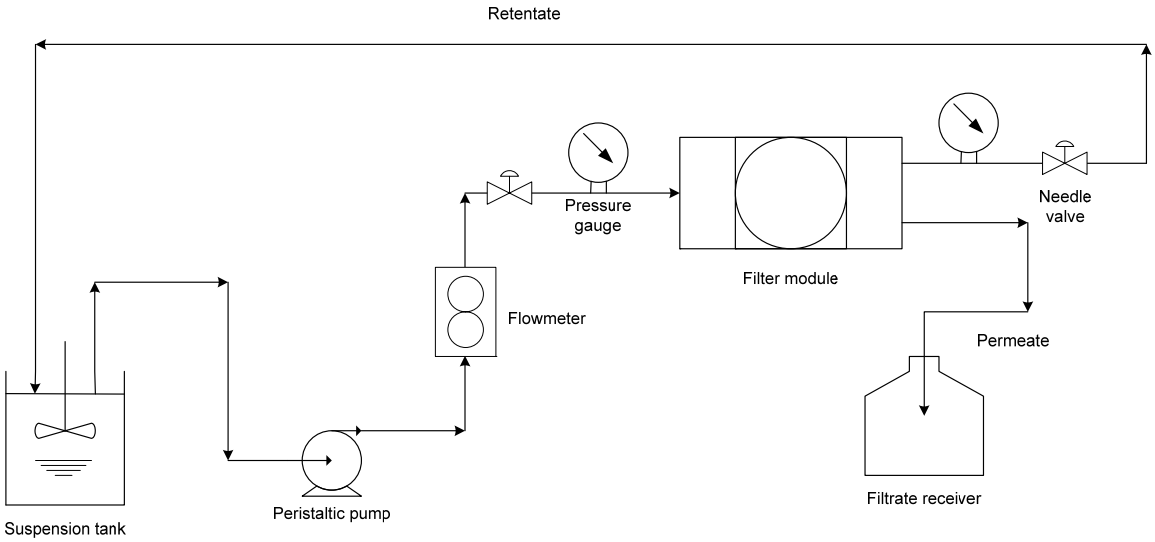

Fig. 1 Schematic diagram of cross-flow microfiltration system

with a cross-flow configuration and an effective area of 7.07×10^{-4} m^2. The setup of this cross-flow filtration test rig is illustrated in Fig. 1. The operating conditions were constant for all the experiments. The TMP and cross-flow velocity (CFV) were maintained at 100 kPa and 0.13 ms^{-1}, respectively. A stirrer in the suspension tank was used to ensure that the cells were evenly distributed in the feed suspension. The suspension was continuously recycled throughout the filtration module by a Masterflex model 7553-79 peristaltic pump (US). Both the concentrated retentate and the permeate were recirculated back to the suspension tank in all experiments. The permeate was collected in a filtrate receiver that was returned back to the suspension tank in order to keep the cell concentration constant.

Upon placement of a membrane in the module, DI water was circulated in the test rig at a TMP of 100 kPa and a CFV of 0.13 ms^{-1} for 5 min before microfiltration experiment with microalgae cells to measure the pure water flux (J_o) for each fresh membrane. J_o across a clean membrane can be expressed in terms of volume of permeate per unit time per unit membrane surface area ($lh^{-1}m^{-2}$). Generally, J_o through a porous membrane in pressure driven processes is directly proportional to the applied hydrostatic pressure, according to Darcy's law (Mulder 1996). Darcy's law states that the solvent passage through the membrane is a function of the applied pressure as follows.

$$J_o = \frac{P_{TM}}{\eta . R_m} \tag{1}$$

where η is the solvent viscosity, R_m is the hydrodynamic resistance of the membrane and P_{TM} is the TMP. R_m is a membrane constant and does not depend on the feed composition or on the applied pressure (Mulder 1996).

During cell separation, membrane performances were evaluated according to the permeate flux,

J ($lh^{-1}m^{-2}$). It was calculated by dividing the permeate volume, ΔV, collected in time period, Δt, by the effective surface area of the membrane, A_e, as follows

$$J = \frac{\Delta V / \Delta t}{A_e} \tag{2}$$

The filtration of the microalgae suspension in all the experiments was performed until the filtration flux reached a steady state (at least 1 h). After each experiment, the system was rinsed with DI water and a new membrane was placed for the next experiment. All the experiments were conducted in triplicates for each membrane.

3. Results and discussion

3.1 Characterization of Chlorella sp.

Chlorella sp. is a unicellular green alga. It is the strain most favored by researches because easily available and easily cultured in the laboratory (Petrusevski *et al.* 1995). Individual *Chlorella* sp. cells are spherical in shape and loosely aggregated (Fig. 2).

The particle size distribution of *Chlorella* sp. is important as it affects the performance of cross-flow filtration. As shown in Fig. 3, one peak was observed in the particle sizes distribution ranged from 2 to 8 μm with a mean size diameter of 3.67 μm as determined by laser diffraction technique.

3.2 MF performances

Test runs using DI water were used to determine initial membrane performances prior to the MF of microalgae cells. Fig. 4 shows the average permeation flux of DI water that was determined experimentally for each material with various pore sizes. CA and CN membranes had the highest water fluxes among all the membranes. These results are related to the hydrophobicity of the fresh membranes, which will be discussed in the next section. CA and CN membranes with large pore diameters (3.0 μm) exhibited the highest water fluxes because filtration flux increases with increasing pore diameter in the absence of fouling. This result can be expected because a higher filtration is caused by increasing pore diameter although in different types of membranes. A similar observation was made by Rossignol *et al.* (1999) when filtering marine microalgae with microfiltration and ultrafiltration membranes.

3.3 Effect of membrane material

Membrane fouling can be characterized by an initial rapid decrease in flux, followed by a long and gradual flux decline (Field *et al.* 1995). The performances of four different MF membrane materials are shown in Fig. 5. All the membranes had pore sizes measuring 0.8 μm. A significant flux decline was observed for the first 10 min, after which a gradual reduction eventually stabilized into the steady state permeation flux. It was observed that the significant flux decline was due to the deposition of microalgae cells on the membrane surface that led to membrane fouling. Despite being made from different materials, the CA and CN membranes showed similar

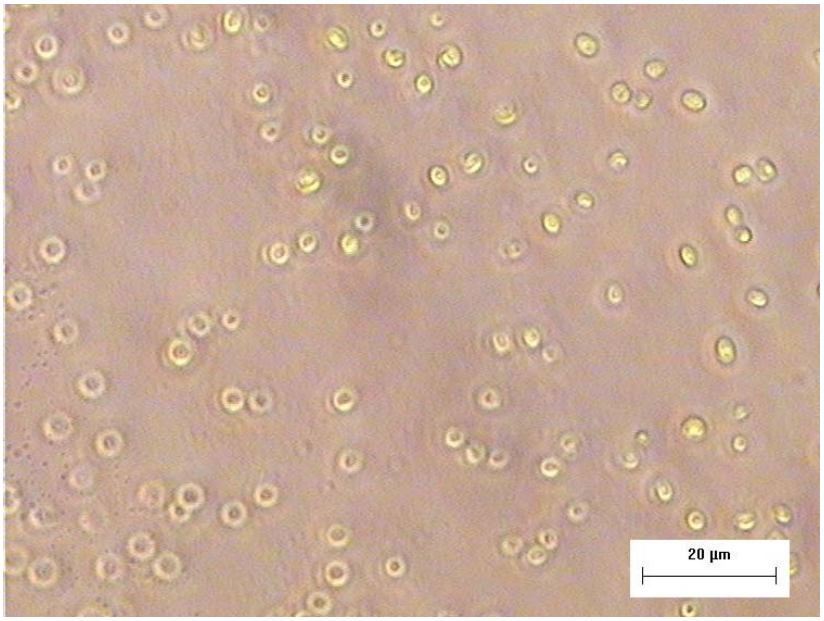

Fig. 2 Optical observation of *Chlorella* sp.cells

permeate flux patterns. After 50 min of operation, the steady state permeation fluxes for both membranes were still very similar and were the highest values attained. The PP membrane ranked a close second while the PVDF membrane had the lowest steady state flux. Flux decline is clearly affected by the membrane material and literature (Ho and Zydney 1999, Dizge *et al.* 2011) suggests that it can also be affected by porosity and roughness of the surface.

Before conducting the MF experiments, the hydrophobicity of each membrane material was determined by measuring the angle between the water (liquid) and membrane (solid). Ahmad *et al.* (2010) reported that a material is deemed hydrophobic if the value of the contact angle is greater than 90°. Thus, the smaller the receding angle, the less hydrophobic, or more hydrophilic the membrane surface.

Before conducting the MF experiments, the hydrophobicity of each membrane material was determined by measuring the angle between the water (liquid) and membrane (solid). Ahmad *et al.* (2010) reported that a material is deemed hydrophobic if the value of the contact angle is greater than 90°. Thus, the smaller the receding angle, the less hydrophobic, or more hydrophilic the membrane surface.

The shapes of the DI water droplets on PP and PVDF membrane surface are shown in Fig. 6. Of the four membranes used in this study, the PVDF membrane had the most hydrophobic surface with a contact angle value of 126.63°.The PP membrane was less hydrophobic with a contact angle value of 95.97°. These angles are much larger than the 0.00° values of the CA and CN membranes (Figures are not shown) that indicate that DI water had almost adsorbed on those surfaces. This means that the CA and CN membranes had the greatest performances due to their hydrophilic nature that allowed them to adsorb DI water much more quickly than the hydrophobic membranes. In addition, DI water droplet is easier to immerse in the membrane and the membrane wettability rate is faster in the hydrophilic surfaces.

Conversely, the PVDF membrane's large contact angle is responsible for its lower permeability. Jung *et al.* (2006) confirmed that the rate of flux decline for the hydrophobic membrane was significantly greater than for the hydrophilic membrane. This phenomenon can be further explained by PVDF's low surface tension values (25 dynescm^{-1}) and lack of active groups in its surface chemistry for the formation of "hydrogen-bonds" with water or aqueous solutions (Ahmad *et al.* 2010).

The significance of the contact angle was also discovered by Gekas *et al*. (1992) and Jonsson and Jonsson (1995). They found that when comparing membranes of different materials, the lower the receding angle, the higher the relative flux and flux recovery at the end of filtration. They also found that the measurements of the receding angle had to be supplemented with measurements of surface roughness and porosity because more open membranes have a higher apparent hydrophilicity due to a higher porosity.

However, the opposite result was observed by Dizge *et al.* (2011) when a CA membrane with a pore size of 0.45 μm showed the most rapid decline in flux compared to polyethersulfone (PES), mixed ester (ME) and polycarbonate (PC) membranes. They also stated that the initial rapid drop of the flux could not be due to the porosity of the membrane, as suggested by Gekas *et al.* (1992), but rather to the irregular and rough surface of the CA membrane. Nevertheless, according to several authors, the rapid flux decline or the lower permeability performance was attributed to the hydrophobic nature of the membrane (Masselin *et al.* 2001, Vaisanen *et al.* 2002).

In terms of steady state permeation flux, the hydrophilic membranes in this study seem to be better choices than the hydrophobic membranes. Thus, the CA and CN membranes need to be compared using another membrane characteristic: pore size.

3.4 Effect of pore size

The effects of the different pore sizes on the permeate fluxes of the CA and CN membranes can be seen in Fig. 7. At the beginning of filtration, flux increased with increasing membrane pore size (CA 0.8 < CA 1.2 < CA 3.0 and CN 0.8 < CN 1.2 < CN 3.0). This implies that most membrane fouling occurred at the entrances of the membrane pores or on the membrane surfaces early in the filtration period. However, after 6 min of operation, the flux was observed to be higher for both CA and CN membranes with a pore size of 1.2 μm (CA 0.8 < CA 3.0 < CA 1.2 and CN 0.8 < CN 3.0 < CN 1.2). The decrease in flux for the membranes with a pore size of 3.0 μm could be the result of pore blocking with microalgae cells.

Table 2 Blocking phenomena in filtration

Type of blocking	Description
Complete blocking	Particle size is larger than that of the membrane pore; particles will deposit on the membrane surface to block the entrances of the membrane pores completely.
Intermediate blocking	The diameter of the particles is almost the same as that of the membrane pores; particles may deposit on the pores entrances or migrate into the pores.
Standard blocking	Particle sizes are smaller than those of the membrane pores; particles are deposited onto the internal pore walls, leading to a decrease in the pore volume.
Cake filtration	This is similar to complete blocking. However, when the concentration of the slurry is high enough, particles may deposit on the membrane surface or on the deposited particle layer to form a filter cake.

Hwang and Lin (2002) described four kinds of blocking phenomena in filtration: 1) complete blocking, 2) intermediate blocking, 3) standard blocking and 4) cake filtration (Table 2). Because the particle size of cells suspension was ranging from 2 to 8 μm with mean size diameter of microalgae cells is 3.67 μm (Fig. 3), the blocking of the 3.0 μm pores falls under the category of intermediate blocking. Microalgae cells could settle on other surface cells that were already blocking some pores or they could also directly block some membrane areas. In complete blocking, the cells can still block the entrances of the membrane pores completely, but the larger cells cannot block the internal pore walls as they have decreased in diameter, allowing only the solution from microalgae cells to pass through the membrane. This phenomenon can be proved via the characterization of the membrane surfaces before and after MF.

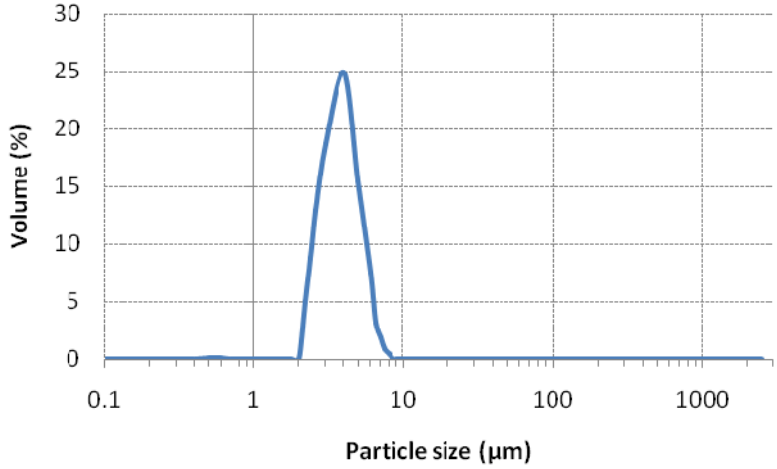

Fig. 3 Particle size distribution of *Chlorella* sp. (wavelength = 830 nm)

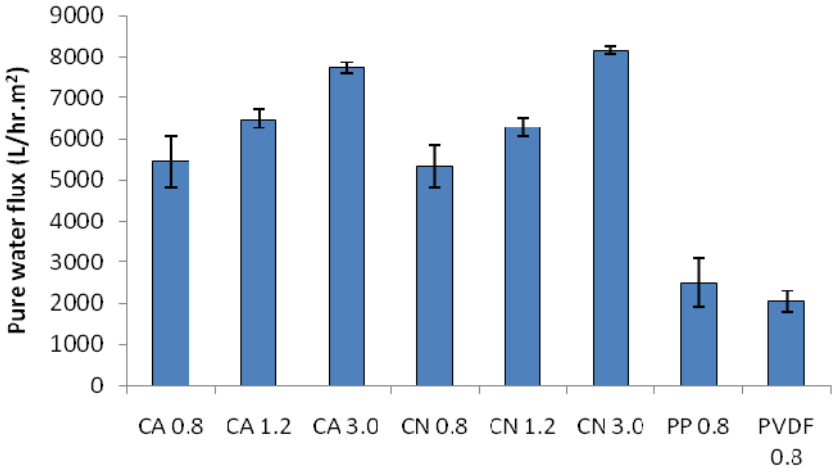

Fig. 4 Pure water flux of membranes (TMP = 100 kPa; CFV = 0.13 ms^{-1})

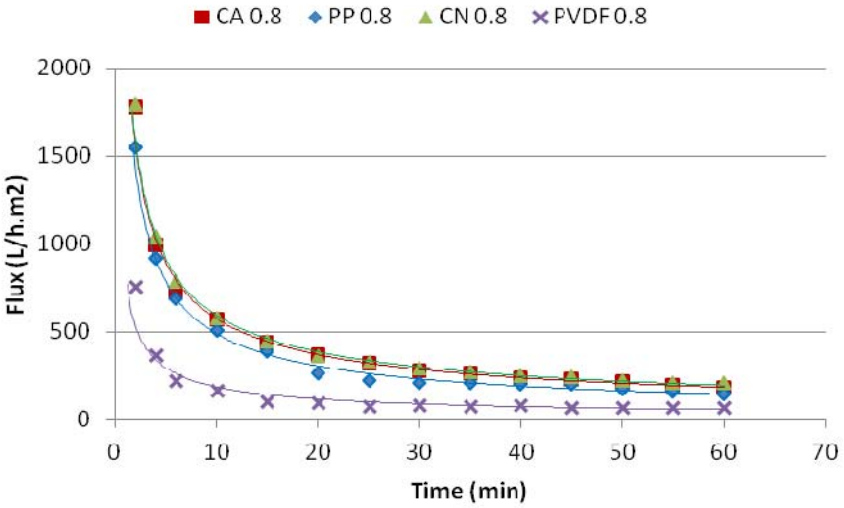

Fig. 5 Effect of membrane material on microfiltration performance (TMP = 100 kPa; CFV = 0.13 ms^{-1})

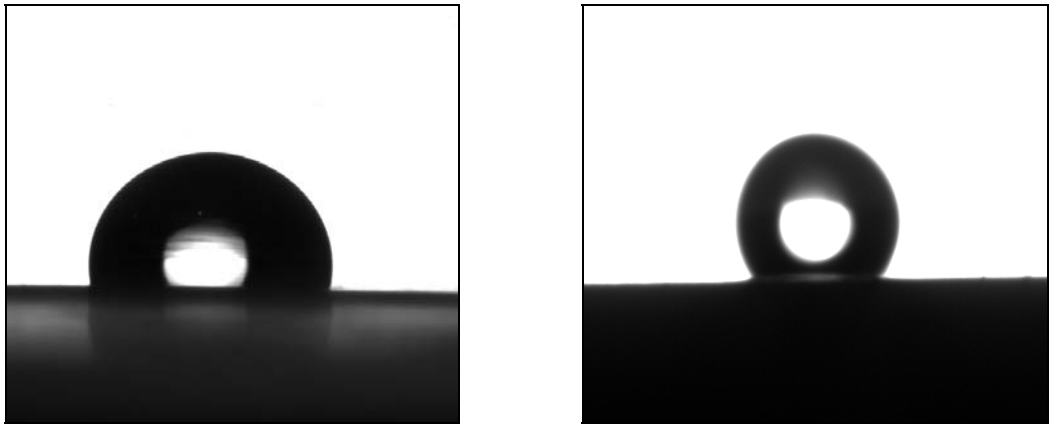

(a) (b)

Fig. 6 Optical images of a water droplet on the membrane surface: (a) PP 0.8 μm and (b) PVDF 0.8 μm

There are a number of methods to characterize the membrane pore structure. SEM is one of the most popular methods that provide two-dimensional images of surfaces. The SEM images for the fresh and fouled CA membranes with pore sizes of 1.2 and 3.0 μm are presented in Fig. 8 and Fig. 9. Figs. 8(a) and 9(a) show SEM images of the fresh membrane surfaces. Although the CA membrane has a very rough surface with irregular pores, it has a relatively flat surface with surface pore sizes greater than the nominal pore size of the membrane. Comparing the SEM images shown in Figs. 8(b) and 9(b), the cells were deposited on the membrane surface, leading to a reduction in the pore diameter; therefore, increasing the filtration resistance. However, a few cells in Fig. 8(b) were carried by the retentate across the membrane surfaces and did not foul the interior of the pores. The rapid flux decline is mainly due to the membrane pore size reduction at the pore entrances. Thus, the mean pore size of the fouled membrane was reduced to only 30-60% of the

original size due to the fouling of the cells. The opposite image was observed in Fig. 9(b) where the cells adsorbed onto the membrane pore walls, therefore, clogging the interior of the pores and thus, the membrane resistance is increased quickly and lowest filtration rate could be obtained. Because the size of the membrane pores was almost equivalent to that of cells, a few cells may have migrated into the membrane pores, whereas others deposited on the pore entrances. This phenomenon can also be classified as intermediate blocking of cells (Hwang and Lin 2002). This blocking would be transform into cake filtration after 10 min of MF and larger cake resistance occurred, thus, resulting in a reduction of permeate flux compared to the membranes with pores size of 1.2 μm. In addition, the microfiltration with large pore diameters was more sensitive to fouling (pore clogging), which probably increased with the presence of cell fragments and debris that produced a cake layer that caused irreversible fouling (Rossi *et al.* 2004).

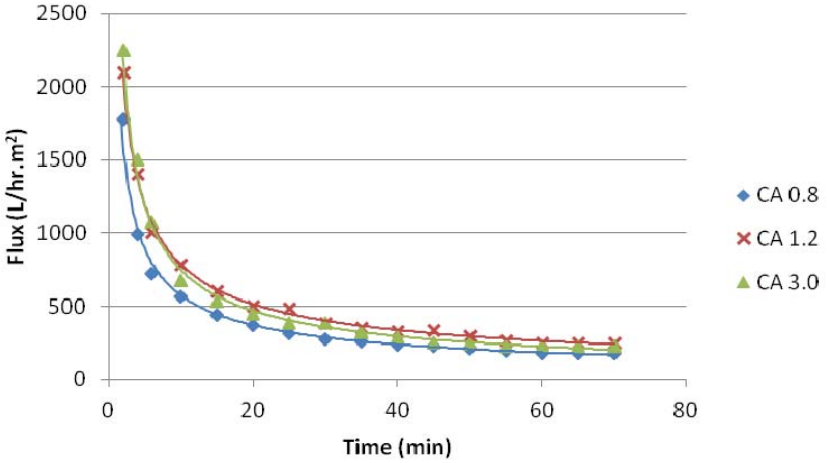

(a)

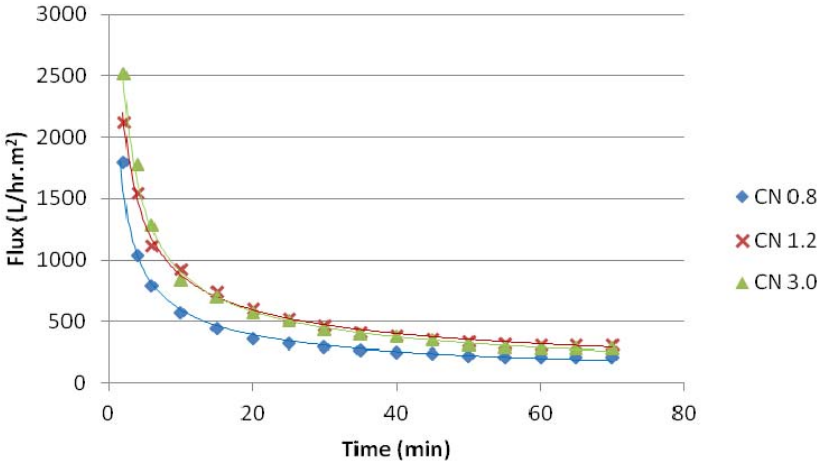

(b)

Fig. 7 Effect of pore size on microfiltration performance for (a) CA; and (b) CN membranes (TMP = 100 kPa; CFV = 0.13 ms^{-1})

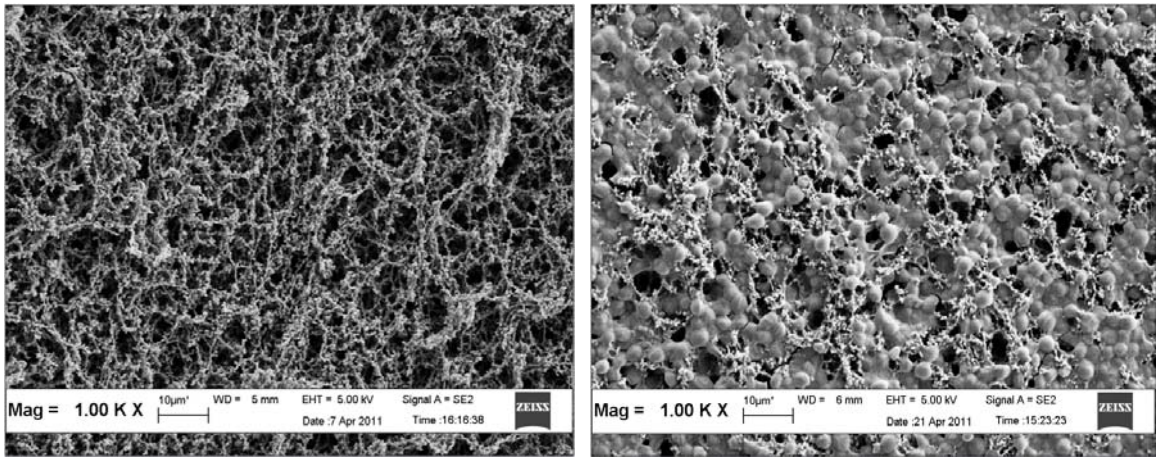

(a) (b)

Fig. 8 SEM images of CA membrane with pore size of 1.2 μm at 60 min of filtration: (a) fresh membrane; and (b) fouled membrane

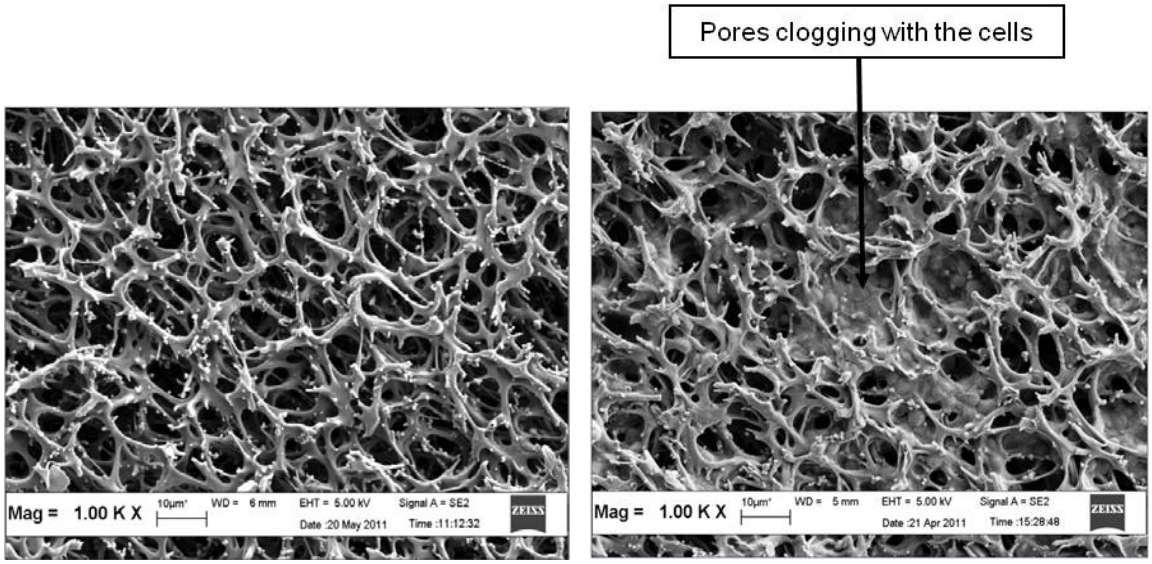

(a) (b)

Fig. 9 SEM images of CA membrane with pore size of 3.0 μm at 60 min of filtration: (a) fresh membrane and (b) fouled membrane

4. Conclusions

The flux decline behavior of microalgae separation in cross-flow MF was studied using four different membrane materials: CA, CN, PP and PVDF. The reduction in permeate flux was dependent on the type of membrane material. The hydrophilicity of the membrane, determined from contact angle measurements, was also an important factor affecting flux. The CA and CN membranes, with contact angles of 0.00° had the greatest performances in terms of steady state

permeation flux. The PP and PVDF membranes had contact angle values of 95.97° and 126.63°, respectively. CA and CN membranes with three pore sizes were compared to evaluate the efficiency of these hydrophilic membranes. Although the pure water flux increased with increasing the pore size diameter (0.8 < 1.2 < 3.0 μm), optimum performances were obtained from membranes with a pore size of 1.2 μm when filtering a foulant suspension. The increase in membrane pore diameter in MF promotes pore plugging that contributes to intermediate blocking. The pore blocking on the membrane surfaces were observed using SEM images. All these membrane characteristics led us to conclude that the hydrophilic CA and CN membranes with a pore size of 1.2 μm exhibited the best performances in term of permeation flux.

Acknowledgements

The research described in this paper was financially supported by USM Research University (RU) Grant (Grant No. 1001/PJKIMIA/814060) and (Grant No. 1001/PJKIMIA/811165), USM Postgraduate Research Grant (Grant No. 1001/JKIMIA/8044014) and USM Membrane Science and Technology Cluster. The authors are very grateful to Mr. Rashid Selamat for assisting with the SEM measurements. N.H. Mat Yasin gratefully acknowledges Universiti Malaysia Pahang (SLAB 2011) for the scholarship.

References

Ahmad, A.L., Mat Yasin, N.H., Derek, C.J.C. and Lim, J.K. (2011), "Optimization of microalgae coagulation process using chitosan", *Chem. Eng. J.*, **173**(3), 879-882.

Ahmad, A.L., Mat Yasin, N.H., Derek, C.J.C. and Lim, J.K. (2012), "Crossflow microfiltration of microalgae biomass for biofuel production", *Desalination*, **302**, 65-70.

Ahmad, A.L., Sunarti, A.R., Lee, K.T. and Fernando, W.J.N. (2010), "CO_2 removal using membrane gas absorption", *I.J. Greenhouse Gas Control*, **4**, 495-498.

Babel, S. and Takizawa, S. (2010), "Microfiltration membrane fouling and cake behavior during algal filtration", *Desalination*, **261**, 46-51.

Dizge, N., Soydemir, G., Karagunduz, A. and Keskinler, B. (2011), "Influence of type and pore size of membranes on cross flow microfiltration of biological suspension", *J. Membrane Science*, **366**(1-2), 278-285.

Field, R.W., Wu, D., Howell, J.A. and Gupta, B.B. (1995), "Critical flux concept for microfiltration fouling", *J. Membrane Science*, **100**, 259-272.

Gekas, V., Persson, K.M., Wablgren, M. and Sivik, B. (1992), "Contact angles of ultrafiltration membranes and their possible correlation to membrane performance", *J. Membrane Science*, **72**, 293-302.

Ho, C-C. and Zydney, A.L. (1999), "Effect of membrane morphology on the initial rate of protein fouling during microfiltration", *J. Membrane Science*, **155**, 261-275.

Hwang, K-J. and Huang, P-S. (2009), "Cross-flow microfiltration of dilute macromolecular suspension", *Separation and Purification Technology*, **68**, 328-334.

Hwang, K-J. and Lin, T-T. (2002), "Effect of morphology of polymeric membrane on the performance of cross-flow microfiltration", *J. Membrane Science*, **199**, 41-52.

Hwang, K-J. and Sz, P-Y. (2010), "Filtration characteristics and membrane fouling in cross-flow microfiltration of BSA/dextran binary suspension", *J. Membrane Science*, **347**, 75-82.

Jaouen, P., Vandanjon, L. and Quemeneur, F. (1999), "The shear stress of microalgal cell suspensions (*Tetraselmis suecica*) in tangential flow filtration systems: the role of pumps", *Desalination*, **68**, 149-154.

Jonsson, C. and Jonsson, A-S. (1995), "Influence of the membrane material on the adsorptive fouling of ultrafiltration membranes", *J. Membrane Science*, **108**, 79-87.

Jung, C-W., Son, H-J. and Kang, L-S. (2006), "Effects of membrane material and pretreatment coagulation on membrane fouling: fouling mechanism and NOM removal", *Desalination*, **197**, 154-164.

Krstic, D.M., Markov, S.L. and Tekic, M.N. (2001), "Membrane fouling during cross-flow microfiltration of *Polyporus squamosus* fermentation broth", *Biochem. Eng. J*., **9**, 103-109.

Lim, J. K., Derek, C.J.C., Jalak, S.A., Toh, P.Y., Mat Yasin, N.H., Ng, B.W. and Ahmad, A.L. (2012), "Rapid magnetophoretic separation of microalgae", *Small*, **8(11)**, 1683-1692.

Makardij, A., Chen, X.D. and Farid, M.M. (1999), "Microfiltration and ultrafiltration of milk: Some aspects of fouling and cleaning", *Trans IChemE Part C*, **77**, 107-113.

Masselin, I., Durand-Bourlier, L., Laine, J.M., Chassray, P.Y. and Lemordant, D. (2001), "Membrane characteristic using microscopic image analysis", *J. Membrane Science*, **186**, 85-96.

Mulder, M. (1996), *Basic Principles of Membrane Technology*, 2nd edition, Kluwer Academic Publishers, Dordrecht, The Netherlands, pp. 427.

Pearce, G. (July-August 2007), "Introduction to membranes: Fouling control", *Filtration & Separation*, **44(6)**, 30-32.

Petrusevski, B., Bolier, G., Van Breemen, A.N. and Alaerts, G.J. (1995), "Tangential flow filtration: A method to concentrate freshwater algae", *Wat. Res*., **29(5)**, 1419-1424.

Rossi, N., Derouiniot-Chaplain, M., Jaouen, P., Legentilhomme, P. and Petit, I. (2008), "*Arthrospira platensis* harvesting with membranes: Fouling phenomenon with limiting and critical flux", *Bioresource Technology*, **99**, 6162-6167.

Rossi, N., Jaouen, P., Legentilhomme, P. and Petit, I. (2004), "Harvesting of *Cyanobacterium arthrospira platensis* using organic filtration membranes", *Food Bioproducts Processing*, **82**, 244-250.

Rossignol, N., Vandanjon, L., Jaouen, P. and Quemeneur F. (1999), "Membrane technology for the continuous separation microalgae/culture medium: compared performances of cross-flow microfiltration and ultrafiltration", *Aquacultural Engineering,* **20**, 191-208.

Vaisanen, P., Bird, M.R. and Nystrom, M. (2002), "Treatment of UF membranes with simple and formulated cleaning agents", *Trans IChemE Part C*, **80**, 98-108.

CC